UPTEC X 06 024
APR 2006
ISSN 1401-2138

LARS ANDERS CARLSON

On the feasibility of nuclear fusion experiments with XUV and X-ray free-electron lasers

Master’s degree project

UPPSALA UNIVERSITET

Molecular Biotechnology Programme

Uppsala University School of Engineering

UPTEC X 06 0024	**Date of issue 2006-04**

Author

Lars Anders Carlson

Title (English)

On the feasibility of nuclear fusion experiments with XUV and X-ray free-electron lasers

Title (Swedish)

Abstract

We have performed simulations to investigate the feasibility of deuterium-deuterium nuclear fusion experiments with novel X-ray and extreme ultraviolet free-electron lasers. Two cases were considered: First, using the existing FLASH facility at DESY (Hamburg) to irradiate a bulk target such as deuterated plastic or a metal deuteride. This scenario is studied using the plasma physics software Cretin. Secondly, the case of using molecular clusters as a target for the hard X-ray FEL is investigated with molecular dynamics simulations. Our results indicate that a solid target irradiated by the FLASH would not be heated enough, whereas molecular clusters irradiated by a hard X-ray FEL would produce the neccessary keV deuterons.

Keywords

free-electron lasers, plasma physics, molecular dynamics, nuclear fusion

Supervisors

Nicusor Timneanu
Department of Cell and Molecular Biology, Uppsala universitet

Scientific reviewer

Janos Hajdu
Department of Cell and Molecular Biology, Uppsala universitet

Project name	Sponsors
Language **English**	Security **Secret until 2007-05**
ISSN 1401-2138	Classification
Supplementary bibliographical information	Pages **35**

Biology Education Centre Biomedical Center Husargatan 3 Uppsala
Box 592 S-75124 Uppsala Tel +46 (0)18 4710000 Fax +46 (0)18 555217

On the feasibility of nuclear fusion experiments with XUV and X-ray free-electron lasers

Lars Anders Carlson

Sammanfattning

Bakgrunden till det här examensarbetet är utvecklingen av *frielektronlasrar*, en radikalt ny typ av forskningsanläggning kapabel att producera röntgenblixtar som är tusen gånger kortare och en miljon gånger starkare än vad dagens modernaste anläggningar genererar.

Jag har använt teoretiska modeller och datorsimuleringar för att undersöka möjligheten att använda planerade och existerande frielektronlasrar till kärnfusionsexperiment. Kärnfusion uppstår när vissa typer av atomkärnor kolliderar med tillräckligt hög hastighet och smälter samman i en energiproducerande reaktion. Fusion med tungt väte har t ex föreslagits för framtida "rena" kärnkraftverk. Fusionsexperiment med frielektronlasrar skulle vara principiellt intressant som en ny kategori av experiment.

Två hypotetiska experiment simulerades: I det första skulle den existerande ultravioletta frielektronlasern i Hamburg användas för att bestråla ett fast ämne innehållande tungt väte (deuterium). Resultaten antyder i det här fallet att de studerade deuteriuminnehållande ämnena inte skulle nå den nödvändiga temperaturen på ca tio miljoner °C. Den andra experimentidén var att använda planerade röntgenfrielektronlasrar, som kommer stå färdiga i Stanford 2009 och Hamburg 2012, för att bestråla deuteriuminnehållande små droppar (*kluster*) bestående av nån handfull upp till några tusental molekyler. Här indikerar simuleringarna att kluster av tungt vatten, D_2O, skulle explodera tillräckligt våldsamt för att kunna generera kärnfusion.

Examensarbete 20p Civilingenjörsprogrammet Molekylär bioteknik

Uppsala universitet april 2006

Contents

1 Introduction

Nuclear fusion remains one of the big hopes for a clean and abundant source of energy, and this is a busy time for fusion research. Several major fusion research facilities are being planned or constructed today, the ITER reactor [1] in France being one and the National Ignition Facility [2] in the USA another. In addition to this, compact and powerful pulsed optical/IR lasers have made possible new types of "table-top" fusion experiments.

Here, we wish to examine a new possibility for nuclear fusion research. We have investigated what types of deuterium-deuterium fusion experiments might be feasible with X-ray and extreme ultraviolet (XUV) free-electron lasers (FELs). This new type of radiation sources will provide pulses that are orders of magnitude more intense and shorter than what today's synchrotrons provide. The FLASH facility (formerly known as VUVFEL) [3] in Hamburg currently operates at 32 nm, and hard X-rays from an FEL will be available at the LCLS in Stanford in 2009. Despite the radically new properties of these facilities, there is no record in the literature on whether they could be used for fusion research. Recognising this window of opportunity, we will consider two hypothetical FEL-based fusion experiments: irradiating a deuterium-containing solid target with the FLASH, and irradiating molecular clusters with a pulse from a hard X-ray FEL.

The basic requirement for fusion to occur is that a sufficient number of light nuclei, at a sufficiently high density, reach high kinetic energies during a sufficiently long time. Thus, the question to be asked here, regardless of the type of experimental setup, will be: What is the kinetic energy distribution of the deuterons, and how long will it stay that way? Anything put into the focus of an intense FEL beam will quickly ionise and turn into plasma, so plasma physics is one of the starting points for our thinking. Irradiating a solid, the ions will aquire their kinetic energy from Coulomb collisions with the free electrons, which in turn are produced and heated by the laser pulse. Thus, estimations of the electron gas temperature will be crucial. In the clusters being ionised, structural relaxation effects, through Coulomb explosion, will determine the velocity distributions, which makes molecular dynamics an appropriate simulation method.

1.1 Nuclear fusion

For the sake of this study, nuclear fusion could simply be viewed as a reaction taking place between two colliding atomic nuclei, with a probability depending on their kinetic energy and the geometry of their collision. Yet, spending some time going through the basic concepts of nuclear physics will greatly enhance the understanding of these phenomena. A general introduction to nuclear fusion can be found e.g. in the first chapter of [4].

The basic equation underlying the energetics of nuclear physics is the expression for the energy contained in a resting mass

$$E = mc^2, \tag{1}$$

derived from the more general expression of special relativity,

$$E^2 = m^2c^4 + \mathbf{p}^2c^2. \tag{2}$$

These equations express the equivalence of mass and energy, which is dramatically apparent in nuclear reactions. Looking at the masses of atomic nuclei, it is apparent that all nuclei are actually lighter than the sum of their constituent protons and neutrons. This *mass defect* Δm is given by

$$\Delta m = Zm_p + (A - Z)m_n - m, \tag{3}$$

where Z is the number of protons, m_p the mass of the proton, $(A-Z)$ its number of neutrons, m_n the mass of the neutron and m is the mass of the nucleus. Using equation (1) one then obtains the binding energy B of the nucleus as

$$B = \Delta mc^2 \tag{4}$$

which is the energy that would be required in order to split the nucleus in its protons and neutrons. This energy is typically expressed in MeV or GeV. A useful quantity when comparing the stability of nuclei is the *binding energy per nucleon*, B/A. Plotting this quantity against the mass number A, one observes that it has a maximum (corresponding to a maximum stability) around $A = 56$, with areas of lesser stability for larger and smaller values of A. This is the basis for both nuclear fission and fusion, since nuclei can split or combine to reach more stable conformations. Nuclei with $A < 56$ will tend to fuse, whereas nuclei with $A > 56$ will tend to split in order to reach the most stable configuration. The thermodynamics of a nuclear reaction is expressed in terms of its Q-value

$$Q = \sum B_{final} - \sum B_{initial}, \tag{5}$$

being simply the energy absorbed or released in the reaction.

1.2 Cross-sections, reaction rates and yields

The cross-section is a central concept in both theoretical and experimental physics, and, being an observable, it is often the meeting point of the two. It expresses the probability of a reaction between two or more species, given the geometry and kinetics of their collision. Consider a general reaction between the species A and B

$$A + B \longrightarrow C + D, \tag{6}$$

where the species collide and form the reaction products C and D. Consider the reaction in the rest frame of the species A, of which there are N_A at a density n_A (low enough for absorption effects to be negligible). Let there be a constant flux of B particles at Φ_B per unit time and unit area incident on the A particles. The number of reactions $\dot{N}_C = \dot{N}_D$ per unit time is expressed using the *cross-section* σ as

$$\dot{N}_C = \sigma N_A \Phi_B \tag{7}$$

or

$$\sigma = \frac{\dot{N}_C}{N_A \Phi_B}. \tag{8}$$

reaction	**Q (MeV)**	**σ@10 keV (barn)**	**σ@100 keV (barn)**	**σ_{max} (barn)**	**ϵ_{max} (keV)**	
$p + p \longrightarrow D + e^+ + \nu$	1.44	$(3.6 * 10^{-26})$	$(4.4 * 10^{-25})$			(pp)
$p + D \longrightarrow {}^3He + \gamma$	5.49					(pD)
$D + D \longrightarrow {}^3He + n$	3.27	$2.78 * 10^{-4}$	$3.7 * 10^{-2}$	0.11	1750	(DD1)
$D + D \longrightarrow T + p$	4.04	$2.81 * 10^{-4}$	$3.3 * 10^{-2}$	0.096	1250	(DD2)
$D + T \longrightarrow {}^4He + n$	17.59	$2.72 * 10^{-2}$	3.43	5.0	64	(DT)
$T + T \longrightarrow {}^4He + 2n$	11.33	$7.90 * 10^{-4}$	$3.4 * 10^{-2}$	0.16	1000	(TT)

Table 1: Fusion reactions between hydrogen isotopes. ϵ_{max} is the energy at which σ obtain its maximum value σ_{max}. All energies are centre-of-mass kinetic energies. Data from [4].

From this, it is clear that the cross-section has the dimensions of an area, which gives it a pictorial interpretation as the "target size". This definition is also applicable to e.g. absorption and scattering. Cross-sections are often expressed in the unit cm^2 or *barn*, 1 barn $=10^{-24}$ cm^2 $= 10^{-28}$ m^2.

From the velocity of the B particles a *reaction rate* $\langle \sigma v \rangle$ can be calculated. Given the velocity v_B of the particles B, and the cross-section σ, a B particle "sweeps out" a volume σv_B per unit time . Any particle A within this volume will interact with the particle B. So the number of reactions per particle B per unit time is given by

$$\frac{\dot{N}_C}{N_B} = n_A \sigma v_B, \tag{9}$$

σv_B being the reaction rate. If the particles B have a velocity distribution $p(v)$, the reaction rate is given by

$$\langle \sigma v_B \rangle = \int \sigma(v_B) v_B p(v_B) dv_B. \tag{10}$$

The total number of reactions in a volume V during the time τ is thus given by

$$\tau \int_V n_A n_B \langle \sigma(v) v \rangle dV. \tag{11}$$

In a reaction where the species A and B are the same, the resulting yield from a volume V existing for the time τ is

$$\frac{\tau}{2} \int_V n^2 \langle \sigma(v) v \rangle dV \tag{12}$$

where $n = n_A = n_B$.

1.3 Fusion reactions between hydrogen isotopes

As explained above, nuclear fusion is thermodynamically most favourable for the lightest elements. It is not restricted to reactions between hydrogen isotopes, but these are the most important for fusion research and the prospect of energy production. One of the reasons for this is their higher cross-section at comparably low temperatures.

Table 1 summarises the major fusion reactions that occur between protons (p), deuterons (D) and tritions (T). The reaction products include positrons (e^+), photons (γ) and neutrinos (ν). From that data, it is apparent that the DT reaction has the highest cross-section at lower plasma temperatures, which is the reason that a deuterium-tritium mix would be the fuel of choice for a fusion reactor.

For "table top" type fusion experiment, the DD reaction has been used because of its "sufficiently large" cross-section and non-radioactive reactants. This is the reaction that we will consider for possible experiments at FELs. The reactions (DD1) and (DD2) are roughly equally probable at low temperatures, and fusion can be detected through the appearance of 2.45 MeV neutrons from reaction (DD1). Being uncharged, the neutrons could easily escape the reaction volume, as opposed to the charged products of the reactions.

1.4 Large scale fusion experiments: MCF and ICF

One of the ultimate goals for large fusion research facilities is of course to find a viable concept for an energy producing fusion reactor. In this context, ignition and break-even are two neccesary prerequisites. As the name would imply, *ignition* occurs when the fusion reaction produces enough heat to be self-propagating, with no need for external heating. *Break-even* is reached when more energy has been produced by the fusion reaction than what was supplied to start it.

The major problem in achieving ignition and break-even is to keep the DT plasma together for a long enough time. A plasma with a temperature of a few keV (i.e. tens of millions K) would melt any physical container, and so other types of confinement techniques have had to be deviced.

In *magetic confinement fusion* (MCF) [5], a toroidal magnetic field is used to confine the plasma. Due to the Lorentz force

$$\mathbf{F} = q\mathbf{v} \times \mathbf{B} \tag{13}$$

charged particles can only move freely in the direction of the magnetic field lines, bending off on a circular trajectory in the plane perpendicular to the magnetic field. This is how the closed field lines of an MCF reactor keep the plasma confined in a doughnut-shaped volume. The international collaboration project ITER [1], to be built in France, will be an MCF reactor.

In *inertial confinement fusion* (ICF) [4], a different approach is taken. Here, a capsule of DT fuel is heated and compressed by powerful IR lasers irradiating it from all directions. This will ignite the fuel. There is no subsequent mechanism to confine the fusion plasma but the inertia in its expansion, hence the name inertial confinement. Due to this concept, ICF is by necessity a pulsed process. Two major ICF facilities are being constructed today, the National Ignition Facility [2] in the USA and the Laser Méga-Joule [6] in France. It can also be noticed that ICF is the principle behind the H-bomb, where the fuel is compressed and ignited not by lasers but by a "conventional" fission-based nuclear charge.

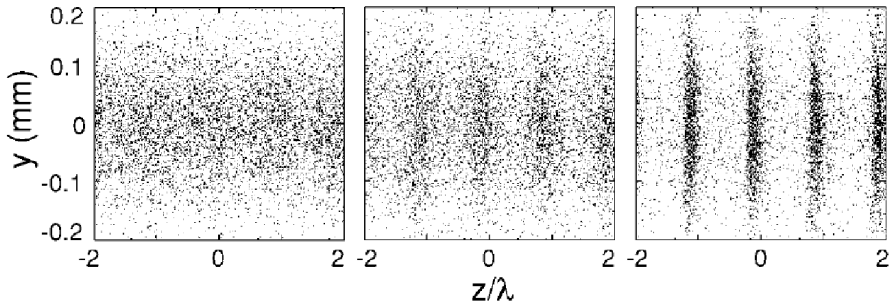

Figure 1: As the electron bunch moves through the long undulator, the developing electric field of the radiation structures the bunch into microbunches. In the structured bunch the electrons radiate in phase with each other, and thus the intensity of the radiation is proportional to the square of the number of electrons, as opposed to the linear proportionality of non-coherent superposition. Image from [7].

1.5 Free-electron lasers and their applications

Despite their name, *free-electron lasers* [7] are not related to regular lasers, who work by stimulated emission. Instead, FELs work along the same principles as synchrotrons [8], i.e. producing radiation from accelerating charges. In a synchrotron, electrons are accelerated to high energies and then led through an *undulator*. This is an array of dipole magnets with switching polarity, which forces the electrons to oscillate in the direction perpendicular to their velocity, thus emitting radiation. Due to relativistic effects present at the high electron energies, the radiation will be emitted in a very narrow cone in the forward direction.

If the undulator were long enough, and the electron bunch travelling through it small and dense enough, the developing electric field of the radiation would interact with the electron bunch and start structuring it into *microbunches* (see 1). This is an effect which can be understood with classical electrodynamics [9], and the basic innovation of an FEL. When the pulse is structured, the radiation from the individual electrons starts to add coherently since every microbunch behaves like a point source. Doing so, the pulse intensity is no longer proportional to the number of electrons N, but to N^2. Except for this major boost in pulse intensity, other pulse properties such as coherence are also affected by this "lasing".

The high requirements that an FEL puts on the electron beam is the reason that linear electron accelerators have to be used instead of synchrotrons, and as mentioned above the undulator has to be five to ten times longer than those found in synchrotrons in order for the microbunching to develop. Since FELs producing vacuum ultraviolet and X-ray radiation are a new concept, what research they can be used for is yet to be seen. The first experiments at 100 nm were done with the Tesla Test Facility (TTF) at DESY in Hamburg, studying the interaction of the intense pulses with noble gas clusters [10]. Lately, the first successful diffraction imaging experiments [11] were done with same facility,

now upgraded to produce 32 nm radiation and carrying the name FLASH. For up-coming soft- and hard X-ray FELs, the planned experiments range from atomic physics and plasma physics to chemistry and structural biology, all taking advantage of the uniquely short and intense radiation pulses from the FELs.

1.6 "Table top" fusion experiments

In a laboratory scale fusion experiment, ignition and break-even are usually not realistic goals. Instead, the goal is to observe and quantify that fusion takes place (usually by observing 2.45 MeV neutrons from the DD1 reaction, see table 1) as a result of exciting the system. Although ingenious set-ups have been deviced using e.g. pyroelectric crystals [12], the vast majority of "table top" fusion experiments utilise pulsed optical/IR lasers to heat the sample. Because of the analogies between these types of experiments and what we will investigate for FELs, we shall consider the principles behind these setups in some more detail.

Pretzler *et al* [13] were able to detect 2.45 MeV neutrons after irradiating a solid target consisting of deuterated polyethylene with a pulsed optical laser. The key element in this experiment was to split the pulse in a smaller first part, creating a *pre-plasma*, and a stronger second part. The second pulse hit the target with a 300 ps delay, and was focussed to an intensity high enough for relativistic effects to occur in the laser-plasma interaction. This *relativistic self-focussing* was enough to heat the target to sufficient temperatures. Except for the relativistic effect, the heating mechanism here basically works along the lines of "classical" plasma physics thinking: the laser heats the electron gas, which through collisions heats the ions in the plasma.

In a milestone work by Ditmire *et al* [14, 15], nuclear fusion was observed when a beam of D_2 clusters was irradiated by a pulsed optical laser. In this case, the heating mechanism is a radically different one. Despite the fact that the photon energy is too low for ionisation through the single photon absorption, at these high intensities and relatively long wavelengths, *field ionisation*[1] will cause a rapid ionisation of the clusters. With the short pulses used, the clusters will be stripped of most of their electrons before having the time to adapt significantly to their new electronic configuration. What follows is that the charged particles will repel each other, leading to the *Coulomb explosion* of the highly charged cluster.

A simple model for the kinetic energy distribution from an exploding cluster can be obtained as follows [17]: We assume that the ionisation of the cluster takes place on a shorter time-scale than its explosion. The kinetic energy of a particle when the cluster has exploded to infinity equals its potential energy before the explosion. Let n be the particle density in the cluster, $\langle q \rangle$ the average charge of a particle and r_{max} the radius of the cluster. Then, the potential energy of a deuteron (with charge e) on the cluster surface is obtained from Coulomb's law

[1] Field ionisation can be understood classically as the electric field of the laser pulse enabling an electron to tunnel out of the potential of the nucleus. The effect can appear when an atom or ion is exposed to an intense laser pulse whose frequency is low compared to the Bohr frequency (see [16], pp. 863-).

as

$$E_{max} = \frac{e\frac{4\pi}{3}r_{max}^3 n\langle q\rangle}{4\pi\epsilon_0 r_{max}} = \frac{en\langle q\rangle r_{max}^2}{3\epsilon_0}. \tag{14}$$

where $\frac{4\pi}{3}r_{max}^3 n\langle q\rangle$ is the total charge of the cluster. The shape of the energy distribution function $p(E)$ is obtaines by using

$$p(r) = 4\pi r^2 n, \quad r \leq r_{max} \tag{15}$$

and (analogous to (14))

$$E(r) = \frac{en\langle q\rangle r^2}{3\epsilon_0} = kr^2 \Leftrightarrow r = \sqrt{\frac{E}{k}} \Rightarrow dr = \frac{dr}{dE}dE = \frac{1}{2\sqrt{kE}}dE \tag{16}$$

to express the distribution as a function of E:

$$p(r)dr = p_r\left(\sqrt{\frac{E}{k}}\right)\frac{1}{2\sqrt{kE}}dE = \frac{2\pi}{k\sqrt{k}}\sqrt{E}dE \tag{17}$$

Thus the kinetic energy distribution from an exploding cluster is in this approximation given by

$$p(E) \propto \sqrt{E}, \quad E \leq E_{max} = \frac{en\langle q\rangle r_{max}^2}{3\epsilon_0}. \tag{18}$$

Continuing along the lines of Ditmire *et al*, Last and Jortner [18, 19] proposed the use of "heteroclusters" of e.g. CH_4 or D_2O. When these explode due to ionisation, a dynamic effect will push the deuteron kinetic energies towards the E_{max} of equation (14), making the distribution more biased towards this value than the $\sqrt{E}$ distribution. This happens because the deuterons would have a higher charge-to-mass ratio than, say, a C^{4+} ion from a CD_4, and thus experience a stronger acceleration than the heavier ions, which they will outrun in the explosion, being repelled by subsequently larger fractions of the cluster. Experimental observations of fusion from heteroclusters were made shortly thereafter by Grillon *et al* [20], and the dynamic acceleration effects have been verified by comparing energy spectra from exploding CH_4 and CD_4 clusters [21].

1.7 Aim of the study

As mentioned above, the aim of the present study is to make an educated guess (simulations) whether novel free-electron lasers could be used for nuclear fusion science. If indications of this could be found, it would be an eye-opener that could tie together two major, today separated, scientific communities: fusion science and FEL science. We have set out to investigate what types of deuterium-deuterium fusion experiments might be feasible with X-ray and extreme ultraviolet (XUV) free-electron lasers. Two types of FEL-based fusion experiments will be considered: irradiating a deuterium-containing solid target with the FLASH, and irradiating molecular clusters with a pulse from a future hard X-ray FEL. In both cases, experimental proof of nuclear fusion reactions would be detection of 2.45 MeV neutrons as a reaction product, so the results of our simulations will be analysed in terms of whether the neutron count would be sufficient.

2 Theoretical models

We have used two different models to simulate the case of a solid or molecular clusters being ionised by an FEL pulse. This is because, as mentioned, the deuterons are expected to be heated through different mechanisms in these two cases. For a solid target, the VUV/XUV pulse will create a plasma, whose electron gas it primarily heats. The ions will then be heated by the electrons through Coulomb collisions. This process is studied using the plasma physics software Cretin [22, 23]. In the case of the clusers being ionised by a hard X-ray pulse, the ions will aquire kinetic energy primarily from the Coulomb explosion. To study this, we have modified a molecular dynamics model from Neutze *et al* [24], implemented in the MD software package GROMACS [25].

2.1 Molecular dynamics

The world of atoms and molecules is the world of quantum mechanics. Only with quantum mecanics can phenomena like tunneling, quantisation of energy levels and wave-particle duality be described correctly. However, solving the time-dependent Schrödinger equation

$$i\hbar\frac{\partial}{\partial t}\Psi(\hat{\mathbf{x}_1},\ldots,\hat{\mathbf{x}}_n,t)=\hat{H}(t)\Psi(\hat{\mathbf{x}}_1,\ldots,\hat{\mathbf{x}}_n,t) \tag{19}$$

for a system like a large cluster of molecules in an intense laser pulse is completely intractable. For this type of problems, a classical approach might give approximate answers.

The basic idea of molecular dynamics (MD) is to treat each atom as a classical particle, and set up a potential energy function $V(\mathbf{x}_1,\ldots,\mathbf{x}_n)$ to describe the interaction of the particles. The dynamics of the system is then solved by choosing initial values for positions and velocities of all atoms, and integrating

$$\begin{cases} \mathbf{F}_i=-\nabla_{\mathbf{x}_i}V(\mathbf{x}_1,\ldots,\mathbf{x}_n) \\ \ddot{\mathbf{x}}_i=\frac{1}{m_i}\mathbf{F}_i. \end{cases} \tag{20}$$

The potential energy function is often referred to as the *force field*, and is chosen to reproduce quantities obtained from experiments or quantum calculations. It usually contains terms modelling electrostatic interaction

$$\sum_{ij}\frac{q_iq_j}{4\pi\epsilon_0 r_{ij}}, \tag{21}$$

covalent bond lengths

$$\sum_i\frac{k}{2}(l_i-l_{0,i})^2, \tag{22}$$

bond angles

$$\sum_i C(\theta_i-\theta_{0,i})^2, \tag{23}$$

van der Waals interactions between non-bonded atoms

$$\sum_{ij}\left(\left(\frac{r_A}{r_{ij}}\right)^{12}-\left(\frac{r_B}{r_{ij}}\right)^{6}\right), \tag{24}$$

torsion angles, etc.

A few remarks can be made as to when classical dynamics is appropriate to describe molecular systems. In general, the quantum effects mentioned above should not be dominating the evolution of the system. Studying a biomolecule at room temperature, the thermal energies are generally too small to excite the electronic wave function. This is a necessary prerequisite, since the potential energy function does not change its form as a function of time in MD. Thermal motions are also small enough for bond vibrations etc to be in the harmonic regime, which justifies the form of the potential function. At the other end of the spectrum, an exploding cluster is a system whose electronic wave function is of course very far from the ground state, and it thus should be hard to make a correct force field. What saves the situation is that the dynamics of the system is so heavily determined by the Coulomb repulsion of the ions, which is easy to model if only the charge density build-up is treated correctly.

For this study, we are interested in the Coulomb explosion of molecular clusters ionised by an intense hard X-ray pulse. In particular, the quantity we are looking for is the velocity distribution of the deuterons after the cluster has exploded. For this purpose, we started with the MD model of Neutze *et al* [24]. This model was implemented in the MD software package GROMACS [25] to study the explosion of protein molecules ionised by an intense X-ray pulse, investigating the possibility of single molecule X-ray diffraction at an X-ray FEL. Thus, the primary interest was in a good description of the not-yet-ionised state and the early stage of the explosion. To obtain this, the harmonic potentials for the bond length was replaced with dissociable Morse potentials

$$V(l) = E_\infty + D_e \left(e^{-2\alpha(l-l_0)} - 2e^{-\alpha(l-l_0)} \right), \tag{25}$$

and added the charges produced by ionisation (of the non-hydrogenic atoms) to the partial charges normally used in MD of proteins. Free electrons generated as photelectrons and Auger electrons by the ionisations were not yet included in the simulation.

This model had three drawbacks for our purpose. The first is that it does not treat the free electrons, but considers them to leave the system instantaneously, which might lead to an exaggerated space charge build-up and an overestimation of the vigour of the Coulomb explosion. Although a model has been developed that includes the free electrons as a classical gas at electrostatic equilibrium with respect to the ions [26], we have not to implemented this code in our simulations due to stability issues. The second is that the hydrogens retained their partial charge of +0.41 throughout the simulation. This was a straightforward implementation that led to negligible errors in the simulations of Neutze *et al*, but being specifically interested in the kinetic energies of the deuterons, this would be a big source of error. The third issue is that the energy terms constraining bond angles are not depending on the bond length. Again, this is probably not a big issue when being primarily interested in a correct description of close-to-intact molecules, but might lead to artefacts for highly dissociated structures. For our purpose, we have changed the MD model by giving the hydrogens the partial charge +1.0 (and thus the oxygen of the D_2O molecules -2.0) and by simply removing the bond angle terms from the poteintial energy function. This will result in a flawed description of the not-yet-ionised cluster,

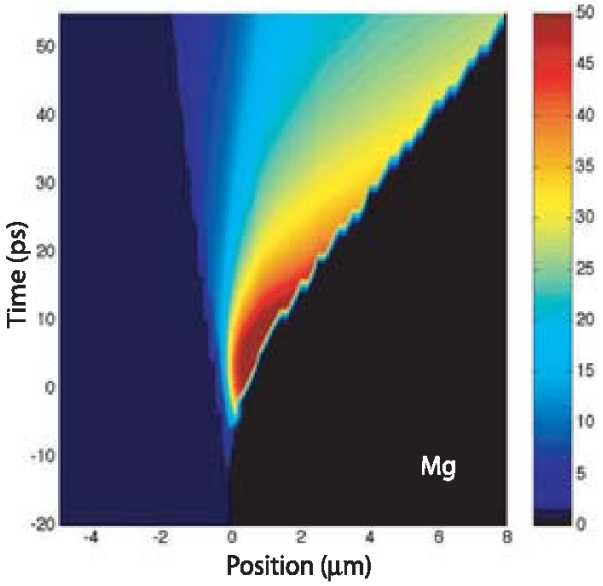

Figure 2: Typical output result of a one-dimensional hydrodynamic simulation of a plasma. Shown is the electron temperature in eV, as a function of position and time, of the electron gas as a solid magnesium sample is irradiated by an intense XUV pulse. Adapted from [27].

but will probably give more correct deuteron velocity distributions at the end of the Coulomb explosion. These will give an upper limit on the deuteron energies.

2.2 Simulations of plasma: hydrodynamics and atomic level kinetics

When studying a macroscopic plasma, the positions and velocities of the individual particles is usually not a fruitful (nor even possible) level of abstraction. Instead, a hydrodynamic description of matter is adopted, representing the plasma by the densities of atoms, ions and electrons as a function of time and possibly position [28]. Applying the continuity equation

$$\frac{\partial n}{\partial t} + \nabla \cdot (n\mathbf{u}) = S, \tag{26}$$

where n is the number density (in e.g. cm^{-3}) of particles of charge q, $\mathbf{u}$ the average velocity (the flux) and S the source function (accounting for ionisations and recombinations), and the momentum-balance equation

$$mn\frac{d\mathbf{u}}{dt} = nq(\mathbf{E} + \mathbf{u} \times \mathbf{B}) - \nabla p - mS\mathbf{u} \tag{27}$$

along with an equation of state such as

$$pV^{\gamma} = const, \tag{28}$$

a description of *one* of the particle types is obtained. However, a complete description of the plasma must also account for the momentum transfer *between* particle types through Coulomb collisions. Figure 2 shows a typical simulation of a metal surface being irradiated by an intense XUV pulse and turning it into a plasma that expands.

To be able to study plasma properties like absorption and emission spectra, a description of state including the population of the excitation levels of the ions is needed. Consider for instance a hypothetical helium plasma, where the neutral He atoms and the He^+ ions can be either in an electronic ground state or in an excited state He^*/He^{+*}. Then, the description of state would have to include populations for all states,

$$\mathbf{n} = \begin{pmatrix} n_{\mathrm{He}} \\ n_{\mathrm{He}^*} \\ n_{\mathrm{He}^+} \\ n_{\mathrm{He}^{+*}} \\ n_{\mathrm{He}^{2+}} \end{pmatrix} \tag{29}$$

(where the n's, again, are densities) along with ion- and electron gas temperatures T_i and T_e and velocities $\mathbf{u}$ for the different species.

To calculate the time dependent population of states, two basic approaches can be distinguished. The first, *local thermodynamic equilibrium* (LTE), amounts to the approximation that every point in the plasma, being characterised by its own temperature, is at thermodynamic equilibrium. Applying statistical mechanics to the population of ionisation and excitation levels, the so called Boltzmann-Saha equations are obtained [29].

In many cases, however, a plasma might be quite far from thermodynamic equilibrium. For instance, if it is irradiated by a strong monochromatic laser pulse, some transitions will be strongly stimulated, leading to the need for *non-LTE* calculations. Non-LTE is the general term for actually calculating populations $\mathbf{n}$ by solving the time-dependent system of equations

$$\dot{\mathbf{n}}(t) = \mathbf{A}(t)\mathbf{n}(t). \tag{30}$$

The matrix $\mathbf{A}$ contains all the rate constants for transitions between the different ionisation and excitation levels, being the the sums of collisional excitations and -ionisations, photoionisations and recombinations. $\mathbf{A}$ depends on the temperature and density of the ions and electrons, and of course on the wavelength and intensity of any radiation. In addition to this, a non-LTE calculation updates the electron gas temperature according to ionisation and recombination rates and the direct interaction between the electron gas and the radiation field (Bremsstrahlung and inverse Bremsstrahlung[2]). The ion gas temperature is then updated according to a simple equilibration model

$$\frac{dT_i}{dt} = C(T_e - T_i), \quad C > 0. \tag{31}$$

Both LTE and non-LTE calculations have in common that they need to be fed an atomic model listing the available levels, their energies and degeneracies,

[2]Bremsstrahlung is the name of the radiation emitted by a charged particle that is decelerated in the electric field of other particles. The inverse process of this is called inverse Bremsstrahlung, and is often the major mechanism by which a laser pulse heats the electron gas of a plasma.

as well as information on how to calculate the rate constants for transitions between the levels. Since hundreds of atomic levels might be populated in a hot plasma at equilibrium, leading to several thousands of transitions to be calculated, there is often a need for a simplified atomic model. The *screened hydrogenic model* is a simplifed atomic model often used in plasma physics, and also in this study. It generates all energy levels by modifying hydrogenic levels with a set of screening coefficients which are simply fitted to experimental data [30, 31]

Another important aspect of plasma physics is the lowering of the ionisation potentials of atoms and ions in a plasma as compared to in vacuum. This effect, called *continuum lowering*, is explained conceptually in appendix B, and its modelling is often crucial for the outcome of plasma physics simulations.

We have used the non-LTE plasma physics software Cretin [22, 23] to simulate the irradiation of solid targets with the FLASH. Cretin can not in itself perform hydrodynamic calculations, but can be used a post-processor to generate detailed spectra, temperatures etc from hydrodynamic simulations. Noting that the highest temperatures in a typical hydrodynamic simulation of this type of processes (see figure 2) are the electron gas temperatures at the surface of the target, we settled for performing zero-dimensional simulations of the surface layer in Cretin.

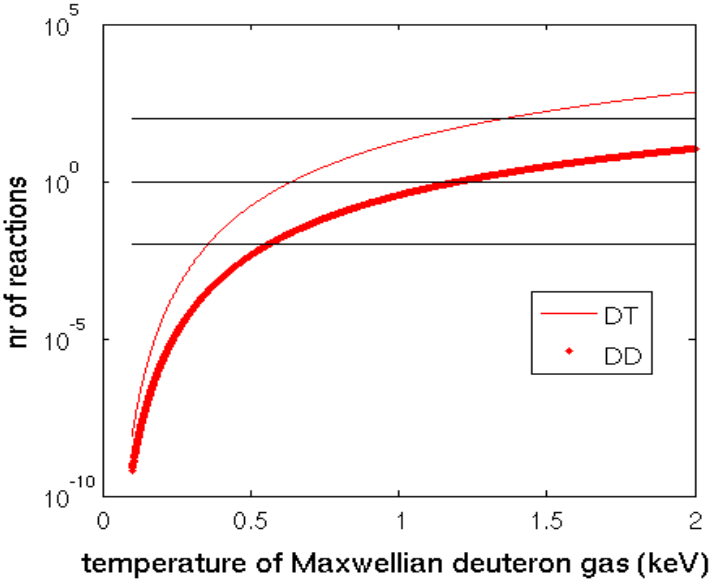

Figure 3: Number of fusion reactions per μm^3 and ps in a deuteron gas with the density of liquid D_2O and Maxwellian velocity distribution, as a function of the temperature in keV. The straight lines correspond to 10^{-2}, 1 and 10^2 reactions. The parametrised reaction rates $\langle\sigma v\rangle(T)$ were taken from [32].

3 Results

3.1 The cross-section: what temperatures are needed?

The ultimate goal of this project is to answer the question: would one be able to detect any 2.45 MeV neutrons (as a result of D-D fusion events) for the considered experiments? Thus, we shall start by looking at what connects the calculated temperatures or velocity distributions and temperatures with this output. This is the reaction rate of equation (10). From [32] we get a parametrisation of the experimentally observed reaction rates as a function of the plasma temperature in keV. This is shown in figure 3, scaled to give the number of reactions per μm^3 and picosecond in a plasma with the deuteron density of liquid D_2O. For reference, the corresponding DT reaction rate is shown.

3.2 Solid targets at the FLASH

The FLASH currently operates at 32 nm, producing pulses with a duration of approximately 30 fs and an energy of up to 20 μJ ($3 * 10^{12}$ photons). In an earlier phase, the facility, then called the Tesla Test Facility (TTF), was operated at 100 nm, producing pulses with an approximate duration of 100 fs. Within two years, it is planned to reach 6 nm. Since this is the only free-electron laser of its kind that is operational already, the obvious first thing to do was to investigate a relatively straight-forward type of experiment using it: irradiating

intensity (W/cm^2)	**photoionisation**	**collisions**	**IBS**	**CL**	**Z@100fs**	**T_e@100 fs (eV)**
$4 * 10^{10}$	yes	yes	yes	yes	3.6	6.7
	yes	yes	yes	no	0.23	3.8
	yes	yes	no	no	0.23	3.8
$2 * 10^{11}$	yes	yes	yes	yes	4.6	8.9
	yes	yes	yes	no	0.46	5.0
	yes	yes	no	no	0.46	5.0
$1.4 * 10^{12}$	yes	yes	yes	yes	5.9	14
	yes	yes	yes	no	0.85	6.7
	yes	yes	no	no	0.84	6.7
$2 * 10^{13}$	yes	yes	yes	yes	8.7	43
	yes	yes	yes	no	1.7	10
	yes	yes	no	yes	6.3	16
	yes	yes	no	no	1.5	9.5
	yes	no	yes	yes	4.0	32
	yes	no	yes	no	0.25	24
$7 * 10^{13}$	yes	yes	yes	yes	12	84
	yes	yes	yes	no	3.8	20
	yes	yes	no	no	2.2	12

Table 2: Simulating the irradiation of Xe clusters by the 100 nm light from TTF. Average ion charge and electron gas temperature at the end of the 100 fs pulse is given. Dependence on pulse intensity and simulation parameters. IBS = inverse Bremsstrahlung heating, CL = continuum lowering according to Stewart and Pyatt [33].

a deuterium-containing solid.

3.2.1 Benchmarking Cretin for the FLASH

Intense laser-plasma interactions have traditionally been studied experimentally at IR wavelengths, simply because no intense source of VUV or shorter wavelength radiation has existed until recently. Thus, Cretin and other plasma simulation tools have been written and tested for a different physical problem than that which we wish to apply it to, which is why we wanted to compare Cretin simulations to experimental data at shorter wavelengths.

The available relevant experimental data is that of Wabnitz *et al* [10]. They used the TTF at 100 nm to irradiate Xe-clusters of varying size, and measured the abundances of ionisation states of the resulting ions, as a function of pulse intensity and cluster size. The measured abundances can be compared to Cretin output. This comparison is also interesting to make because the presence of multiply charged ions, up to +8, in the spectra from the clusters was a very suprising result of the experiment, since the photon energy of 12.7 eV is only enough to ionise single atoms once. The parameter space of this experiment was essentially two-dimensional: in one series, the intensity was kept constant at $2*10^{13}$ W/cm^2, and the cluster size was varied from 1 to $3*10^4$ atoms, and in another the cluster size was kept constant at $\sim$ 1500 atoms while the intensity

was varied between $4 * 10^{10}$ and $7 * 10^{13}$ W/cm^2.

Simulations were done in Cretin of bulk xenon at liquid density being irradiated by a rectangular 100 fs pulse. The Xe density remained constant throughout the simulation, i.e. the onset of the expansion of the clusters was not accounted for. The pulse intensity was varied between $4 * 10^{10}$ and $7 * 10^{13}$ W/cm^2, according to the experiment. By turning off the continuum-lowering, the electron impact excitation and the electron impact ionisation, a "single atom" result is obtained. The inverse Bremsstrahlung heating of the electron gas can also be turned off to investigate its effect in the simulations. Table 2 shows the simulation result in terms of two simple quantities: the average ionisation $\bar{Z}$ and the temperature of the electron gas at the end of the 100 fs pulse. Looking at $\bar{Z}$, it is clear that high average charge states are reached for all simulated intensities. In the experimental spectra, however, multiply charged ions only appeared from the clusters at intensities larger than 10^{12} W/cm^2. With the continuum lowering turned off, Cretin produces more moderate charge states, the population of multiply charged ions (relative to all ions and neutrals) reaching 4%, 16% and 40% for intensities of $2 * 10^{11}$, $1.4 * 10^{12}$ and $2 * 10^{13}$ W/cm^2 respectively.

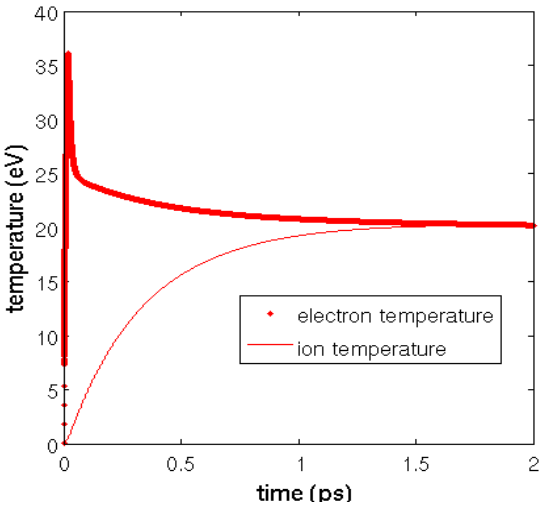

Figure 4: The time evolution of the electron and ion temperatures in MgD_2 following irradiation by a 20 fs FLASH pulse of 32 nm, containing $1.5 * 10^{12}$ photons focussed to a focal radius of 2 μm

3.2.2 Simulating possible targets at 32 nm and 6 nm

We used Cretin to simulate the irradiation of different solids by a single FLASH pulse. The pulse parameters were the current ones at the time of the simulation, i.e. $1.5 * 10^{12}$ photons of 39 eV energy (10 μJ) in a 20 fs pulse. The pulse was modelled as being rectangular. The values in the table are calculated for a focal radius of 20 μm, which gives an intensity of $4*10^{13}$ W/cm^2. This corresponds to the current experimental situation. We also performed calculations corresponding to a tighter focual radius of 2 μm, which would raise the intensity by a factor 100 to $4 * 10^{15}$ W/cm^2. Out of the wealth of time dependent information that Cretin produces, table 3 gives the average charge, $\bar{Z}$, of the heavy atom at the end of the 20 fs pulse, and the ion and electron temperatures at 2 ps, by which time the cold ions have equillibrated with the hot electrons in the simulation (see figure 4 for an example of the time evolution for MgD_2 with a 2 μm focus). Multiphoton effects were turned off in these calculations, but taking them into account had no significant effect at the considered intensities (data not shown). As can be seen from table 3, TiD_2 reaches the highest temperatures of 18 and 92 eV, respectively.

Since the FLASH is planned to eventually reach a wavelength of 6 nm (photon energy of 207 eV), we repeated the 32 nm calculations for 6 nm. As the experimental beam parameters for the future 6 nm operation are unknown, we simply changed the photon energy to 207 eV while keeping the number of photons, the pulse duration and everything else constant. This means that the pulse energy is increased five times. Table 4 shows the same output quantities as table 3 for these runs.

target	**density** ($\mathbf{g/cm^3}$)	$\mathbf{r_{focal}}$ (μ**m**)	$T_{ion}(T_e)$**@2ps (eV)**	$\bar{Z}$**(heavy atom)@20fs**
$LiAlD_4$	0.917	20	0.87(1.2)	0.31
		2	19.7(20.0)	1.0
MgD_2	1.45	20	0.68(1.55)	0.22
		2	20.2(20.2)	1.6
CaD_2	1.70	20	12.7(12.6)	2.9
		2	63.1(63.1)	7.5
D_2O	1.0	20	10.3(10.3)	2.1
		2	58.7(58.7)	4.9
$C_{10}D_{22}$	0.73	20	3.9(3.9)	1.1
		2	50.0(50.7)	3.7
TiD_2	3.75	20	18.2(18.0)	4.1
		2	92.9(91.0)	9.4

Table 3: Results of Cretin runs at 32 nm. The pulse was modelled as being 20 fs long and rectangular, with an intensity corresponding to $1.5 * 10^{12}$ photons in a focal spot with radius 20 and 2 μm, repsectively. The output showed is the electron and ion temperatures after 2 ps, and the charge of the atom which the deuterium is bound to, at the end of the 20 fs pulse. The target densities are taken from [34] and are those of the corresponding hydrides.

target	**density** ($\mathbf{g/cm^3}$)	$\mathbf{r_{focal}}$ (μ**m**)	$T_{ion}(T_e)$**@2ps (eV)**	$\bar{Z}$**(heavy atom)@20fs**
$LiAlD_4$	0.917	20	5.2(5.2)	0.58
		2	42.2(42.6)	4.3
MgD_2	1.45	20	5.5(5.5)	0.42
		2	63.9(63.5)	7.6
CaD_2	1.70	20	14.3(14.3)	1.0
		2	47.3(47.2)	7.2
D_2O	1.0	20	0.83(1.85)	0.32
		2	34.3(34.3)	4.3
$C_{10}D_{22}$	0.73	20	0.11(1.2)	0.15
		2	11.1(11.1)	2.0
TiD_2	3.75	20	2.7(2.7)	1.7
		2	73.7(72.8)	9.4

Table 4: Results of Cretin runs at 6 nm. The calculations were done similarly to those of table 3, only changing the photon energy from 39 eV to 207 eV.

3.2.3 The entire future spectrum of the FLASH for TiD_2

Noticing that titanium deuteride reached the highest temperatures at both ends of the FLASH spectrum, we decided to do a more systematic study of its "temperature landscape" for the entire future wavelength and intensity range of the FLASH. Photon energies were varied between 35 eV and 215 eV, and intensities from 10^{13} to 10^{17} W/cm^2. Pulses were 30 fs long and rectangular. Considering the simple equilibration model for ion heating, the electron gas temperatures at the end of the pulse were use, a value very close to which the ion temperatures would converge. The results are shown in figure 5 for the entire parameter space, and in figure 6 for the subset of runs with $h\nu$=39 eV. They clearly show that a shorter wavelength, at constant intensity, results in lower plasma temperatures.

3.3 Molecular cluster targets at the future X-ray FEL

Using the MD model described in section 2.1, we simulated the Coulomb explosion of D_2O clusters irradiated by a pulse from a hard X-ray FEL. In this case, the heating of the deuterons is not expected to proceed through collisions with a hot electron gas, but rather through structural relaxation (Coulomb explosion) of a rapidly ionised cluster, analogous to experiments by Ditmire *et al* [14]. We assumed a focal radius of 50 nm, and pulses containing between $1 * 10^{11}$ and $3 * 10^{13}$ photons in a pulse length of 10 fs to 100 fs. The actual pulse parameters are of course not available until the first X-ray FEL is running, but these values are close to the estimated parameters. The observable that we have been intersted in is the kinetic energy distribution of the deuterons. Figure 7 shows the build up of kinetic energy during the explosion of a $(D_2O)_{1236}$ cluster, indicating that already in the 10 fs after the pulse maximum, the deuterons have reached high energies. 100 fs after the pulse maximum, there was no significant further increase in energies (data not shown). As figure 8 indicates, if the pulse energy is kept constant, a shorter pulse seems to evoke a more energetic Coulomb explosion. The pulse intensity will also be an improtant factor for the deuteron energies, since it determines the ionisation process. In figure 9 the effect on the energy distribution of varying the number of photons is shown for the $(D_2O)_{1236}$ cluster. We also studied the dependence of the deuteron energy on cluster size. Figure 10 clearly shows, as expected, that larger clusters generate deuterons with higher energies.

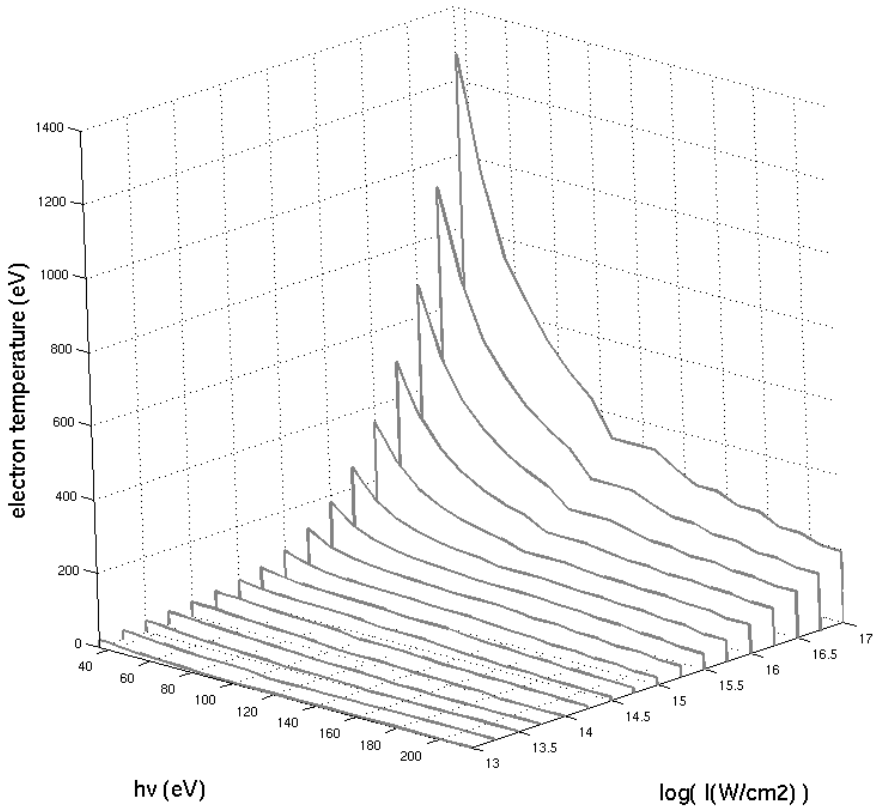

Figure 5: The temperature of the electron gas at the surface of a TiD_2 sample irradiated by a single 30 fs pulse from the FLASH, as a function of photon energy and average pulse intensity.

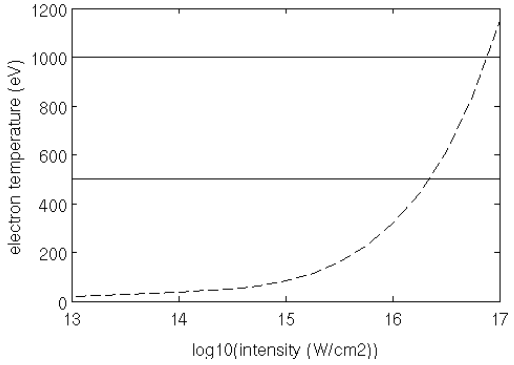

Figure 6: The temperature of the electron gas at the surface of a TiD_2 sample irradiated by a single 30 fs pulse from the FLASH, as a function of pulse intensity. Photon energy is 39 eV.

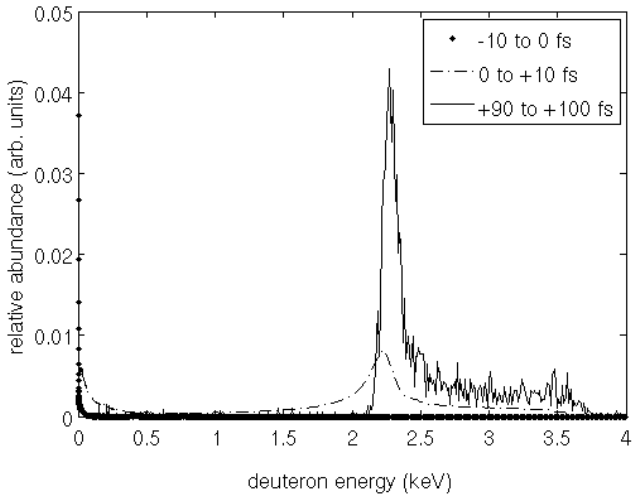

Figure 7: Kinetic energy distributions of the deuterons after the Coulomb explosion of a $(D_2O)_{1236}$ cluster due to ionisation by an X-ray FEL, as a function of time after the pulse peak. Pulse parameters are 10^{13} photons in a 10 fs pulse.

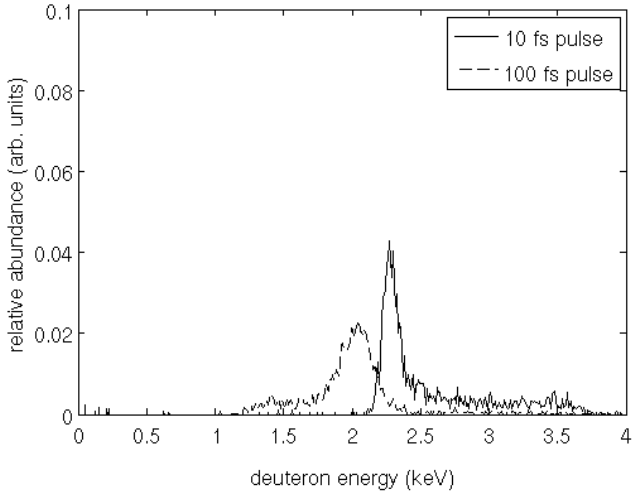

Figure 8: Kinetic energy distributions of the deuterons after the Coulomb explosion of a $(D_2O)_{1236}$ cluster due to ionisation by an X-ray FEL, as a function of pulse length. 10^{13} photons.

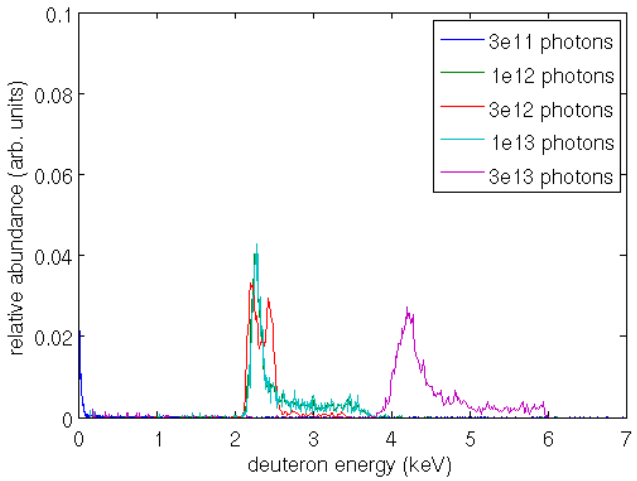

Figure 9: Kinetic energy distributions of the deuterons after the Coulomb explosion of a $(D_2O)_{1236}$ cluster due to ionisation by an X-ray FEL, as a function of the number of photons in the 10 fs pulse.

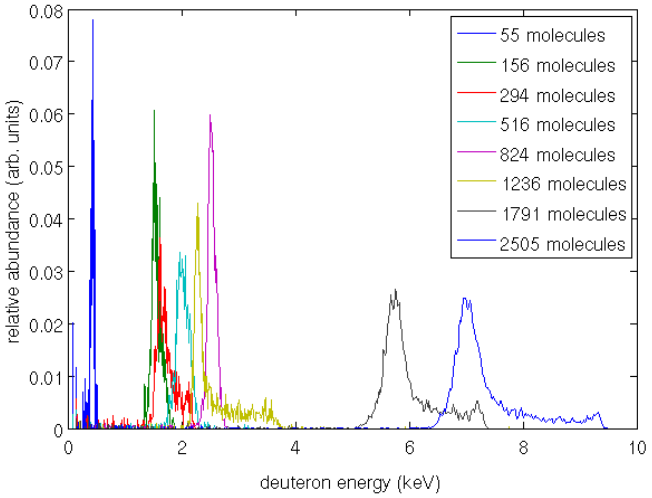

Figure 10: Dependence on cluster size of the kinetic energy distributions of the deuterons after the Coulomb explosion of D_2O clusters due to ionisation by an X-ray FEL. Pulse parameters are 10^{13} photons in a 10 fs pulse. The distributions are calculated for the time interval [+90fs,+100fs] with respect to the pulse peak, by which time the deuterons have practically obtained their maximum velocities.

4 Discussion

The aim of this project was to investigate the possibility of doing nuclear fusion experiments with novel free-electron lasers. These radiation sources produce pulses that contain in the order of 10^{12} photons in roughly 100 fs, which is drastically shorter and more intense than what today's synchrotrons can produce. Because of this leap in performance, there is substantial activity in the scientific community to map out what could be done with these facilities, and proposed experiments reach from biology to atomic physics. Although nuclear fusion is a scientifically and economically very hot topic, and high power visible/IR lasers are regularly used for this type of experiments, there is little notion in the literature on the possibility of doing fusion related work with X-ray FELs.

The condition for fusion to occur is straight-forward, yet difficult to achieve: the nuclei have to reach kinetic energies in the keV range for the fusion cross-section to be significant.

In analogy with other laboratory-scale experiments, we chose to consider the deuterium-deuterium reaction. Compared to the deuterium-tritium reaction, that is the best option for an energy-producing fusion reactor, the DD reaction has a smaller cross-section, but it has the advantage of having only non-radioactive reactants. As an important orientation, the number of reactions to be expected in 1 μm^3 of plasma with D_2O density in 1 ps (in the order of typical plasma parameters, at least for a solid target at the FLASH) is given in figure 3 as a function of deuteron temperature. As the cross-section for Coulomb collisions (leading to thermal equilibration) is larger than that for fusion at all temperatures [28], it is often reasonable to assume that a fusion plasma will have a Maxwellian velocity distribution, and thus to characterise it solely by its temperature. Since the neutrons produced by fusion events will escape the reaction volume isotropically in all directions, at least a few hundred to a few thousand produced neutrons are probably needed in order for a few to hit the detector.

One of the preliminary ideas behind this project was that ionisation on a femtosecond time scale of a material where deuterium was bound to a heavy atom might create repulsion effects ("Coulomb sling") large enough for fusion to occur. An estimation of the order of magnitude of these effects can be given by the potential energy of a deuteron on 1 Å distance from a point charge Ze. This energy, which would be an upper boundary for the kinetic energy of the repelled deuteron, is roughly $14 * Z$ eV, which is too small for our purposes. Thus, one must either turn to materials which are structured so that they have the potential for sufficiently large structural relaxation effects [14, 35] or exploit the standard heating mechanism for plasmas: the pulse heats the free electrons by means of photoionisations and inverse Bremsstrahlung, and the electron gas subsequently heats the ions through Coulomb collisions.

The first experiment we investigated was to use the existing FLASH at DESY (Hamburg) to irradiate a solid deuterium-containing target. The FLASH is planned to work in the 32 nm to 6 nm interval, and currently gives up to $3 * 10^{12}$ photons of 32 nm wavelength in a 30 fs pulse.

We used the non-LTE atomic level kinetics software Cretin [22] to estimate the temperatures at the surface of a solid target irradiated by a single FEL pulse.

This corresponds to the highest temperature that would be obtained in a full one-dimensional hydrodynamic simulation (cf. figure 2), and is thus a short-cut to the relevant information: will the target be heated enough? As targets, we chose to simulate various metal deuterides, deuterated plastic, and D_2O.

Because ultra-intense sources of XUV and X-ray radiation are a novelty, Cretin was developed for simulating interactions between plasma and longer-wavelength lasers, and thus we first needed some type of verification of how it performs for intense short-wavelength pulses. The first and so far only suitable data comes from the experiment by Wabnitz *et al*, where Xe-clusters of varying size were irradiated by intense 100 fs pulses of 98 nm light. The surprising and interesting result of this experiment was the appearance of highly charged ions, up to +8, although the photon energy was only sufficient to ionise isolated Xe atoms once and multi-photon ionisations are believed to be insignificant at these intensities. Thus, the high charge states must be due to the dense environment of the cluster.

We used Cretin to simulate bulk xenon at liquid density being irradiated by a rectangular 100 fs pulse. There is of course a difficulty in comparing these results to the experimental situation of a finite cluster, but bearing this in mind the comparison will still be of interest. By turning off high density effects such as collisional ionisations and continuum lowering, one can compare a "single atom" type result to the full calculation.

Looking at the results for $2 * 10^{13}$ W/cm^2, it is clear that Cretin at least qualitatively reproduces the major result of the experiment: single atoms are only ionised once, atoms in clusters are multiply ionised. For the "single atom" case (continuum lowering and the collisional excitations and -ionisations turned off, lowermost row for $2*10^{13}$ W/cm^2), the average charge of the atoms only reaches 0.25, with virtually no ions having a charge greater than one. With all "density" effects included, the average charge $\bar{Z}$ reaches 8.7. This is a higher value than what can be inferred from the experimental data, where - for large clusters at this pulse intensity - the highest populated charge state is +8, and most of the ions seem to be in a charge state of +3 to +5.

Comparing the Cretin output at different pulse intensities, it is noticeable that high average charge states are reached for all simulated intensities. In the experimental spectra, however, multiply charged ions only appeared from the clusters at intensities larger than 10^{12} W/cm^2. With the continuum lowering turned off, Cretin produces more moderate charge states, the population of multiply charged ions (relative to all ions and neutrals) reaching 4%, 16% and 40% for intensities of $2 * 10^{11}$, $1.4 * 10^{12}$ and $2 * 10^{13}$ W/cm^2 respectively. It has been suspected that the Stewart-Pyatt continuum lowering model exaggerates the ionisations for the early stages in the formation of a dense plasma from a solid [36], and our comparisons seem to be an experimental verification of this problem.

In a later paper from the same group, Laarmann *et al* [37] analysed the energy spectrum of the electrons coming from exploding xenon- and argon clusters ionised by the same source at an intensity of $4.4 * 10^{12}$ W/cm^2. The Xe-clusters in the experiment had an average size of 70 atoms, which makes the comparison with the Cretin runs of bulk Xe more problematic than for the case of the larger clusters of the first paper. Their experimental energy spectra show a thermal

energy distribution with an average electron energy of 10 eV. Comparing this to the Cretin output, one sees that the runs with the continuum lowering effect turned on give higher temperatures, by a factor of 4 to 8, whereas the results with continuum lowering turned off are close to the experimental values.

Turning to the actual simulations at 32 nm (see table 3), it is clear that most of the simulated targets reach low temperatures at $4 * 10^{13}$ W/cm^2. Noteworthy is, that a rule of thumb says that the results of a run are dubious if the average charge $\bar{Z} < 2$, which would disqualify many of these results. At lower ionisations of course the assumption of having free atoms and ions, with corresponding energy levels and cross sections, will also not be a good one, except possibly for the core levels. At the higher intensity of $4 * 10^{15}$ W/cm^2, corresponding to a 2 μm focal radius, especially TiD_2 is heated significantly. Still, a temperature of 93 eV would be too low to be able to observe fusion reactions.

As mentioned, multi-photon ionisation processes were turned off, and turning them on made no difference in these simulations. The fact that the average electron energies in many runs nevertheless exceeds the photon energy of 39 eV is due to the inverse Bremsstrahlung heating of the free electrons. If this process is switched off in Cretin, electron (and thus also ion) energies are strictly below 39 eV for all runs in table 3.

We also simulated the heating process at the shortest wavelength that the FLASH is planned to reach; 6 nm (see table 4). Not having the exact future beam parameters, we simply changed the photon energy, keeping the photon number and the pulsed length of the 32 nm simulations. From these results, it is obvious that higher photon energies do not necessarily mean higher plasma temperatures. The $LiAlD_4$ and MgD_2 samples, which had the lowest temperatures at 32 nm, are heated more by the 207 eV photons, whereas the other samples are actually heated more by the 32 nm pulse. The reason for this can be found in the different dependencies of the electron gas heating on photon energies: the photoelectric effect ($\propto h\nu$) and the inverse Bremsstrahlung heating ($\propto (h\nu)^{-2}$ [38, 39]). In these simulations, the temperatures of several times $h\nu$ can only be achieved through multi-photon processes (which have been seen to be insignificant) or by inverse Bremsstrahlung. Looking at figure 5, the importance of the $(h\nu)^{-2}$ dependence of the inverse Bremsstrahlung absorption coefficient for achieving high temperatures is apparent. The data of figure 6 indicates that intensities of close to 10^{17} W/cm^2 would be needed to heat the TiD_2 sample to 1 keV. 10^{13} photons in 20 fs in a 1 μm focal spot would give an intensity of $9.9 * 10^{16}$ W/cm^2, but this is currently not available.

In the second part of this project, we considered a different way of producing energetic deuterons with an FEL. In analogy with experiments done with pulsed optical lasers [14, 15, 18, 19, 20, 21] we studied the Coulomb explosion of D_2O clusters being ionised by a pulse from an X-ray FEL. The heating mechanism in this case will be a different one than for the solid targets. The pulse will ionise the cluster heavily on a time scale similar to or shorter than the time it takes for the cluster to adapt structurally. Thus, it will suddenly find itself being heavily positively charged (the fast photoelectrons having left the cluster), and will explode as a result of the electrostatic repulsion. For X-rays, it would generally speaking be advantageous to use clusters containing heavy atoms with large cross-sections for photoionisation and short core hole lifetimes. We have

initiated studies of D_2S and deuterium halogenide clusters, but in this study we focussed on D_2O.

From the data shown in figure 7, it is evident that the Coulomb explosion of even a moderately sized cluster of 1236 molecules would produce deuterons of keV energy. The energy build-up seems to occur on a time-scale shorter than 100 fs, and the "dynamic acceleration effect" first predicted by Last and Jortner (see section 1.6 and [18, 19]) is clearly visible in these simulations too.

Next, we studied how the pulse length would affect the deuteron energies. The 10 fs pulse that we used in most simulations, for reasons of stability, is shorter than the 100-200 fs which is expected initially from the LCLS [40] and the European XFEL [41]. However, comparing the resulting energies for a 10 fs and a 100 fs pulse of 10^{13} photons irradiating the $(D_2O)_{1236}$ cluster, the difference is rather small (figure 8). We also studied the dependence of the deuteron energies on pulse intensity (figure 9) and cluster size (figure 10), varying the number of photons from 10^{12} to $3 * 10^{13}$ for the cluster of 1236 molecules, and simulating clusters of 55 to 2505 molecules with a pulse of 10^{13} photons. The expected results that larger clusters and more intensity gives higher energies are verified by these results. It is also clear that the resulting keV energies are achieved robustly with respect to the simulation parameters.

One weakness when using these results for quantitative discussions is that our MD model assumes that all photoelectrons and Auger electrons leave the cluster immediately. The Auger electrons will not have enough kinetic energy to do so, and this leads to an overestimation of the charge density in the cluster. However, this is not likely to change the result by orders of magnitude, but rather by a factor less than two, and the simulations are, as mentioned, otherwise robust with respect to changes in cluster size, pulse intensity and pulse length.

To summarise, we have investigated two possible scenarios for performing nuclear fusion research with novel short-wavelength free-electron lasers. Fusion research is a field of very large scientific and economic interest. Thus, any opportunity to establish a new class of nuclear fusion experiments has a very large potential impact. Our results indicate that irradiating a solid target with a pulse from the existing FLASH facility will not heat it enough, but that molecular cluster targets at the coming hard X-ray lasers have the potential for generating deuterons of keV energy. Hopefully, this report can also serve as a mind-opener and a basis for further discussions in what is still a far from mapped-out terrain.

5 Acknowledgements

Big thank you's go out to my supervisor Nicuşor Tîmneanu for all support and help, and to my co-supervisor Magnus Bergh who taught me Cretin and a lot of plasma physics. Tack så mycket! Thank you Janos Hajdu for inspiration and encouragement, and everyone else in the group for helping out with various things and for making my time here so interesting.

A Debye screening, Debye length and the definition of a plasma

In a plasma, the Coulomb potential of a point charge is altered. The charged particles surrounding a given point charge will adjust so as to minimise their potential energy, and this will lead to a dampening of the potential. This *Debye screening* (sometimes discussed as Debye-Hückel theory) is an important effect in plasma physics, and is for instance one of the ways of explaining the continuum lowering effect of a plasma. It is derived considering a fully ionised plasma being Boltzmann distributed around a fixed point charge q.

The energy of a charged particle in the plasma is classically given by:

$$E = \frac{1}{2}mv^2 + q\Phi(x) \tag{32}$$

where Φ is the electrical potential. The probability for a particle to be found at a point $\mathbf{x}$ with the velocity $\mathbf{v}$ is then given by

$$P(x, v) \propto e^{-\frac{m\mathbf{v}^2/2 + q\Phi(\mathbf{x})}{kT}} \tag{33}$$

or with the velocity integrated out

$$P(x) \propto e^{-\frac{q\Phi(\mathbf{x})}{kT}} \tag{34}$$

This is the distribution that causes the screening of the point charge q. If the electron density in the plasma "far away" from the point charge is $n_{e,\infty}$ and the density of the ions, having charge $+Ze$, is $n_{j,\infty} = n_{e,\infty}/Z$, we have

$$n_e(\mathbf{x}) = n_{e,\infty} e^{\frac{e\Phi(\mathbf{x})}{kT_e}} \tag{35}$$

$$Zn_j(\mathbf{x}) = n_{e,\infty} e^{-\frac{Ze\Phi(\mathbf{x})}{kT_j}}. \tag{36}$$

The net charge density is thus given by

$$\rho(\mathbf{x}) = e(Zn_j(\mathbf{x}) - n_e(\mathbf{x})) = en_{e,\infty}(e^{-\frac{Ze\Phi(\mathbf{x})}{kT_j}} - e^{\frac{e\Phi((x))}{kT_e}}). \tag{37}$$

The electric potential $\Phi(\mathbf{x})$ is obtained through the Poisson equation

$$\nabla^2\Phi(\mathbf{x}) = -\frac{\rho(\mathbf{x})}{\epsilon_0}, \tag{38}$$

which will have a spherically symmetric solution for the potential around our fixed point charge. Inserting the expression for the charge density (37), the *Poisson-Boltzmann equation* is obtained:

$$\nabla^2\Phi(\mathbf{x}) = \frac{en_{e,\infty}}{\epsilon_0}(e^{-Ze\Phi(\mathbf{x})/kT_j} - e^{e\Phi(\mathbf{x})/kT_e}). \tag{39}$$

Solutions for small values of $\Phi(\mathbf{x})$ (i.e. not too close to the point charge) can be obtained through the *Debye approximation*. This approximation amounts to

Taylor expanding the exponentials in the expression for ρ, and keeping the two first terms, out of which the constants cancel, giving

$$\rho(\mathbf{x}) \approx -n_{e,\infty}(\frac{Ze\Phi}{kT_j} + \frac{e\Phi}{kT_e}). \tag{40}$$

Inserting this in (39) gives

$$\nabla^2\Phi(\mathbf{x}) = \lambda_d^2\Phi(\mathbf{x}). \tag{41}$$

with the *Debye length* λ_d defined as

$$\lambda_d = \sqrt{\frac{\epsilon_0 kT_e}{n_{e,\infty}e^2(1 + ZT_e/T_j)}}. \tag{42}$$

In spherical polar coordinates the equation turns into

$$\frac{d^2\Phi}{dr^2} + \frac{2}{r}\frac{d\Phi}{dr} = \lambda_d^2\Phi \tag{43}$$

for a spherically symmetric Φ. The general solution to this equation is given by

$$\Phi(r) = A\frac{e^{-r/\lambda_d}}{r} + B\frac{e^{r/\lambda_d}}{r} \tag{44}$$

where B must be zero for the solution to be physically acceptable for large r, resulting in the *Debye-Hückel potential*

$$\Phi(r) = \frac{qe^{-r/\lambda_d}}{4\pi\epsilon_0 r} \tag{45}$$

from a point charge q, at a "large enough" distance from q. The plasma thus modifies the Coulomb potential by an exponential dampening term. For this statistical treatment to be valid, the particle density in the plasma must be such that there are many particles within a *Debye sphere* of the volume $\frac{4}{3}\pi\lambda_d^3$. This condition, which can be expressed approximately as

$$n_e\lambda_d^3 \gg 1 \tag{46}$$

is also chosen to be the formal *definition* of a plasma.

B Lowering of the ionisation potential in plasmas

It takes less energy to ionise an atom or an ion in a plasma than in vacuum. The model adopted to describe this effect, called *continuum lowering*, is often crucial for the simulation of a plasma. Although there are sophisticated theories for continuum lowering, the principle can be understood starting from the Debye screening presented in appendix A [29]. Part of the energy that needs to be supplied to an atom or an ion in order to ionise it is simply required for separating the negative electron from the positive ion. This energy will be lowered in a plasma which screens the Coulomb potential. More elaborate models for continuum lowering take e.g. electron degeneracy into account, such as the Stewart-Pyatt model [33] that was used for the simulations in this study.

C Glossary

eV	1 eV(electron volt) = $1.6 * 10^{-19}$ J. A temperature of 1 eV (1 k_BT = 1 eV) is roughly 11600 K.
nucleon	Proton or neutron
deuterium	Heavy hydrogen whose nucleus consists of one proton and one neutron. Not radioactive.
tritium	Heavy hydrogen, whose nucleus consists of one proton and two neutrons. Radioactive.
plasma	Ionised gas.
Bremsstrahlung	Radiation emitted by a charged particle that is decelerated in the electric field of other particles
inverse Bremsstrahlung	The inverse process of Bremsstrahlung. Absorption of radiation by charged particles in a plasma.
Debye screening	Screening of a electric charges which occurs in plasmas.
Debye length	Characteristic length of the exponential dampening of the Coulomb potential which is the result of Debye screening.
LTE	Local thermodynamic eqillibrium. Assumption that the population of ions over excitation and ionisation levels is at equilibrium, which allows one to calculate the distributions using statistical mechanics.
non-LTE	Refers to calculating populations by solving the linear system of equations, i. e. not assuming equilibrium.
continuum lowering	The lowering of ionisation potentials that occurs in a plasma due to screening effects.
FEL	Free electron-laser.
MCF	Magnetic confinement fusion.
ICF	Inertial confinement fusion.
neutrino	Uncharged elementary particle with zero or extremely low mass.
positron	The positive antiparticle of the electron.
VUV	Vacuum ultraviolet. Ultraviolet radiation with a wavelength shorter than 200 nm, below which radiation is absorbed in air.
XUV	Extreme ultraviolet. Roughly the wavelength interval 100 nm to 10 nm.
soft X-ray	Roughly the wavelength interval 10 nm to 1 nm.
hard X-ray	Radiation with a wavelength shorter than roughly 1 nm.
FLASH	Short for *f*ree-electron *la*ser in *H*amburg. The FEL at DESY (Hamburg), currently producing 32 nm radiation but designated to reach down to 6 nm.
cluster	Microscopic "droplet" of two or more atoms or molecules, held together by weak forces.

References

[1] http://www.iter.org.

[2] http://www.llnl.gov/nif.

[3] V. Ayvazyan *et al.* Generation of GW radiation pulses from a VUV free-electron laser operating in the femtosecond regime. *Phys. Rev. Lett.*, 88(10):104802, 2002.

[4] S. Atenzi and J. Meyer–ter–Vehn. *The Physics of Inertial Fusion.* Oxford University Press, 2004.

[5] E. Teller, editor. *Fusion. Volume 1: Magnetic Confinement, part A and B.* Academic press, 1981.

[6] http://www-lmj.cea.fr/.

[7] J. Feldhaus, J. Arthur, and J.B. Hastings. X-ray free-electron lasers. *J. Phys. B.*, 38(9):799–819, 2005.

[8] J. Als-Nielsen and D. McMorrow. *Elements of Modern X-Ray Physics.* John Wiley & Sons, Ltd, 2001.

[9] W. Greiner. *Klassische Elektrodynamik.* Verlag Harri Deutsch, 2002.

[10] H. Wabnitz *et al.* Multiple ionization of atom clusters by intense soft X-rays from a free-electron laser. *Nature*, 420(6915):482–485, 2002.

[11] H. N. Chapman *et al.* Ultrafast coherent diffraction imaging with a soft X-ray free-elctron laser. submitted.

[12] B. Naranjo, J.K. Gimzewski, and S. Putterman. Observation of nuclear fusion driven by a pyroelectric crystal. *Nature*, 434(7037):1115–1117, 2005.

[13] G. Pretzler *et al.* Neutron production by 200 mJ ultrashort laser pulses. *Phys. Rev. E*, 58(1):1165–1168, 1998.

[14] T. Ditmire *et al.* Nuclear fusion from explosions of femtosecond laser-heated deuterium clusters. *Nature*, 398(6727):489–492, 1999.

[15] T. Ditmire *et al.* Nuclear fusion in gases of deuterium clusters heated with a femtosecond laser. *Phys. Plasmas*, 7(5):1993–1998, 2000.

[16] B. H. Brandsen and C. J. Joachain. *Physics of Atoms and Molecules.* Pearson Education, 2003.

[17] J. Zweiback *et al.* Nuclear fusion driven by coulomb explosion of large deuterium clusters. *Phys. Rev. Lett.*, 84(12):2634–2637, 2000.

[18] I. Last and J. Jortner. Nuclear fusion induced by Coulomb explosion of heteronuclear clusters. *Phys. Rev. Lett.*, 87(3):033401, 2001.

[19] I. Last and J. Jortner. Nuclear fusion driven by Coulomb explosion of homonuclear and heteronuclear deuterium- and tritium-containing clusters. *Phys. Rev. A*, 64(6):063201, 2001.

[20] G. Grillon *et al.* Deuterium-deuterium fusion dynamics in low-density molecular-cluster jets irradiated by intense ultrafast laser pulses. *Phys. Rev. Lett.*, 89(6):065005, 2002.

[21] M. Hohenberger *et al.* Dynamic acceleration effects in explosions of laser-irradiated heteronuclear clusters. *Phys. Rev. Lett.*, 95(19):195003, 2005.

[22] H.A. Scott. Cretin - a radiative transfer capability for laboratory plasmas. *J. Quant. Spectr. Rad. Transf.*, 71(2–6):689–701, 2001.

[23] H.A. Scott and R.W. Mayle. GLF - A Simulation Code for X-Ray Lasers. *Appl. Phys. B*, 58(1):35–43, 1994.

[24] R Neutze *et al.* Potential for biomolecular imaging with femtosecond X-ray pulses. *Nature*, 406(6797):752–757, 2000.

[25] D. van der Spoel *et al.* GROMACS: Fast, Flexible and Free. *J. Comput. Chem.*, 26(16):1701–1718, 2005.

[26] Magnus Bergh, Nicuşor Tîmneanu, and D. van der Spoel. Model for the dynamics of a water cluster in an x-ray free electron laser beam. *Phys. Rev. E*, 70(5):051904, 2004.

[27] M. Fajardo, P. Zeitoun, and J.C. Gauthier. Hydrodynamic simulation of XUV laser-produced plasmas. *Eur. Phys. J. D*, 29(1):69–76, 2004.

[28] R. J. Goldston and P. H. Rutherford. *Introduction to Plasma Physics.* Institute of Physics Publishing, 1997.

[29] H. R. Griem. *Principles of Plasma Spectroscopy.* Cambridge University Press, 2005.

[30] R. M. More. ELECTRONIC ENERGY-LEVELS IN DENSE PLASMAS. *J. Quant. Spectr. Rad. Transf.*, 27(3):345–377, 1982.

[31] G. Faussurier, C. Blancard, and A. Decoster. NEW SCREENING COEFFICIENTS FOR THE HYDROGENIC ION MODEL INCLUDING l-SPLITTING FOR THE FAST CALCULATION OF ATOMIC STRUCTURE IN PLASMAS. *J. Quant. Spectr. Rad. Transf.*, 58(2):233–260, 1997.

[32] J.D. Huba. NRL PLASMA FORMULARY. Technical report, Naval Research Laboratory, Washington, DC, 2004.

[33] J. C. Stewart and K. D. Pyatt, Jr. Lowering of ionization potentials in plasmas. *Astrophys. J.*, 144(3):1203–1211, 1966.

[34] D. R. Lide, editor. *CRC Handbook of Chemistry and Physics.* CRC Press, 1996.

[35] H. Schwoerer *et al.* Laser-plasma acceleration of quasi-monoenergetic protons from microstructured targets. *Nature*, 439(9):445–448, 2006.

[36] H.-K. Chung, W.L. Morgan, and R.W. Lee. POPULATION KINETICS MODELLING FOR NON-LTE AND NON-MAXWELLIAN PLASMAS GENERATED IN FINITE TEMPERATURE DENSE MATTER EXPERIMENTS ARISING FROM SHORT PULSE X-RAY SOURCES. In *Inertial Fusion Sciences and Applications*, pages 303–306. American Nuclear Society, 2004.

[37] T. Laarmann *et al.* Emission of Thermally Activated Electrons from Rare Gas Clusters Irradiated with Intense VUV Light Pulses from a Free Electron Laser. *Phys. Rev. Lett*, 95(6):063402, 2005.

[38] J. Dawson and C. Oberman. High-Frequency Conductivity and the Emission and Absorption Coefficients of a Fully Ionized Plasma. *Phys. Fluids*, 5(5):517–524, 1962.

[39] T. W. Johnston and J. M. Dawson. Correct values for high-frequency power absorption by inverse bremsstrahlung in plasmas. *Phys. Fluids*, 16(5):722, 1973.

[40] http://www-ssrl.slac.stanford.edu/lcls.

[41] http://xfel.desy.de.